Why are some boundary currents blocked by the equator?

Doron Nof*

Abstract—Existing nonlinear theories for the effect of the equator on northward-flowing boundary jets adjacent to a finite depth upper layer suggest that such inertial currents can flow from the southern to the northern hemisphere with the equator playing no special role (ANDERSON and MOORE, 1979, *Deep-Sea Research*, **26**, 1–22). It is demonstrated in this paper that, in contrast to these flows, nonlinear currents bounded by a front on their open ocean side (i.e. no adjacent upper layer) experience traumatic changes in their structure as they approach the equator. Within a deformation radius away from the equator, they separate from the coast and turn eastward to form a swift narrow jet. The equator blocks their advancement into the northern hemisphere.

The above behavior is demonstrated by examining two nonlinear analytical models. First, we consider a simple highly idealized 1½ layer model of a (southern hemisphere) wedge-like boundary current flowing northward with a wall on its left and a front on its right (looking downstream). It is almost a trivial matter to demonstrate analytically that such a current (which is just a special case of the Anderson and Moore flow) cannot penetrate into the northern hemisphere. Instead, it must separate from the coast in the vicinity of the equator. Secondly, a more realistic and more complicated 2½ layer model is considered. In this nonlinear analytical model the current consists of two active layers. As in the previous model, the core of the current is a wedge-like layer (i.e. it is bounded by a front on the oceanic side) but the remaining surrounding field (i.e. the second moving layer) extends to infinity.

It is shown that the flow in the second layer can cross the equator without any traumatic changes (as suggested by ANDERSON and MOORE, 1979), but the core must again separate from the coast in the vicinity of the equator. As in the previous model, the current associated with the core is blocked by the equator. The general picture of the 2½ layers is then of an initial two-layer inertial boundary current flowing toward the equator in the southern hemisphere. In the immediate vicinity of the equator the current splits into two branches. One separates from the coast and turns eastward whereas the other continues flowing northward until it ultimately reaches its own mid-latitude separation point.

Possible application of this theory to the New Guinea Coastal Undercurrent is briefly discussed. This current turns offshore at the equator as predicted by our model.

1. INTRODUCTION

ENCOUNTERS between meridional currents and the equator are inevitable because of the geography of the oceans. Evidently, the influence that such encounters have on the currents varies from one ocean to another. In the Indian Ocean, the Somali Current crosses the equator with no apparent changes in its structure. ANDERSON and MOORE

---

*Commonwealth Scientific and Industrial Research Organization, Marine Laboratories, Division of Oceanography, Hobart, Tasmania, Australia. Permanent affiliation: Department of Oceanography, The Florida State University, Tallahassee, FL 32306-3048, U.S.A.
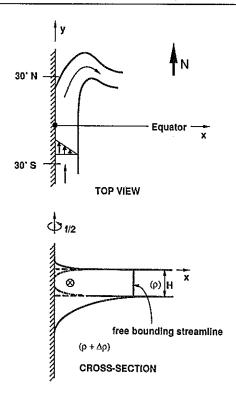
Fig. 1. Schematic diagram of the ANDERSON and MOORE (1979) jet. The inertial jet originates in the southern hemisphere, crosses the equator with no apparent difficulty and then separates from the left wall at mid-latitude. The current is geostrophic in the cross-stream direction. In the cross-section, solid lines correspond to the surface and interface in the southern hemisphere, dashed lines correspond to the surface and interface along the equator, and the dashed–dotted lines illustrate the situation in the northern hemisphere. The current crosses the equator because of the finite depth on the right-hand side (H). Separation occurs in mid-latitude where the near-wall depth vanishes (see text).

(1979, hereafter referred to as AM) have demonstrated that such an equatorial crossing probably corresponds to an inertial jet which occupies a fraction of the upper layer (Fig. 1). In contrast, observations of the New Guinea Undercurrent (TSUCHIYA, 1968; LINDSTROM *et al.*, 1987; ROUGERIE, 1969) suggest that in the Pacific Ocean the equator somehow blocks the northward advancement of the current (Fig. 2).

In this paper a theoretical attempt will be made to explain why the equatorial Pacific is blocking the advancement of the New Guinea Undercurrent. It will be shown that different currents respond very differently to the presence of the equator. In particular, we shall demonstrate that currents bounded by a front on the ocean side can *never* cross the equator, as appears to be the case in the Pacific Ocean (Fig. 2).
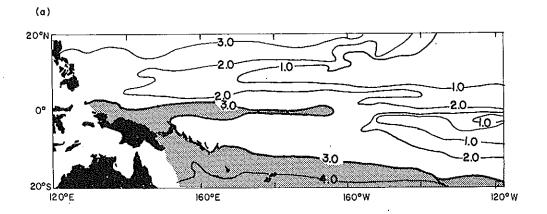
Background

For general information regarding equatorial dynamics the reader is referred to the review articles of McCREARY (1985), ERIKSEN and KATZ (1987) and PHILANDER (1985). As mentioned, from a dynamical point of view, the study that is most closely related to the

problem at hand is that of AM. They addressed an inviscid northward-flowing jet bounded by a wall on the left (looking downstream) and a free streamline (Fig. 1), beyond which the ocean is stagnant, on the right. Analytical and numerical computations indicate that the current crosses the equator with no apparent difficulty. Ultimately, as the current proceeds northward, its near-wall depth vanishes at some (mid) latitude and, at this point, the current leaves the coast and meanders into the interior. The study of CSANADY (1985) also has some relevance to our problem. He discusses an equatorial intrusion-return flow pattern that interacts with a northern water mass; Csanady applies his analysis to the western equatorial Atlantic. The reader is also referred to KAWASE (1987) which discusses the interactions of linear flows with the equator and eastern boundaries and shows that flows generated by Kelvin waves cannot cross the equator.

Methods

The approach that will be taken in this study is similar to that taken in classical jet studies. Namely, we shall examine the detailed behavior of the upstream and downstream
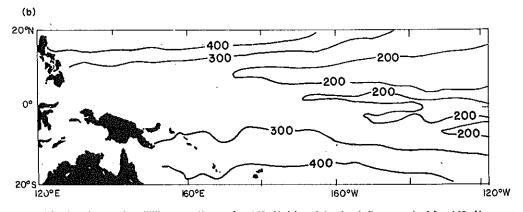
(a)

(b)

Fig. 2.   Oxygen in milliliters per liter at $\delta = 160$ cl/t (a) and the depth (in meters) of $\delta = 160$ cl/t (b). Adapted from TSUCHIYA (1968). Shaded area corresponds to the New Guinea Coastal Undercurrent. The pattern suggests that the equator blocks the northward advancements of the current which is in disagreement with the ANDERSON and MOORE (1979) model (Fig. 1).
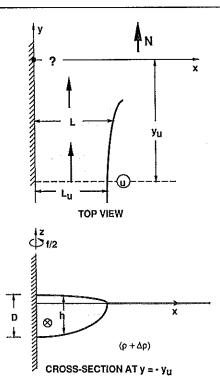
Fig. 3. Schematic diagram of the frontal 1½ layer model under study; the model consists of a single current approaching the equator from the south. The question that we are trying to answer is whether or not the frontal current can cross the equator. The total depth is h; D is the near-wall depth upstream [i.e. $D = h_w(y_u)$, where the subscripts "w" and "u" denote "wall" and "upstream", respectively]. Note that, mathematically, there is no difference between the surface current shown above and an intermediate current sandwiched between two infinitely deep inert layers (not shown).

currents several deformation radii away from the equator and then connect the regions via conservation of mass, momentum, energy and potential vorticity. For clarity, we shall first examine the behavior of a zero potential vorticity, single moving layer model (Section 2). The current is bounded by a wall on the left and a front on the ocean side; it flows northward and approaches the equator from the south (Fig. 3). It is almost a trivial matter to show analytically that such a current cannot exist in the northern hemisphere; i.e. upon reaching the equator it must leave the coast and flow eastward. After presenting this, relatively simple, model we turn to a more realistic and more complicated model of two moving layers (Section 3). In this model the core of the current is again bounded by a front on the ocean side but now the current is embedded in a northward-flowing layer of infinite extent. Using a perturbation scheme it is demonstrated that such adjacent northward-flowing currents can exist in both hemispheres. Despite this aspect, however, it is possible to show that such a system cannot cross the equator as one unit. Instead, a bifurcation is established (Section 4).

2. ONE-AND-A-HALF LAYER MODEL

Impossibility of penetration into the northern hemisphere

In this subsection we shall demonstrate that a northward-flowing jet with a front on the ocean side (Fig. 3) cannot exist in the northern hemisphere. To show this, it is noted that our frontal jet is merely a special case of the AM jet with $H = 0$ (see the cross-section in Fig. 3) and that the jet is in geostrophic balance in the cross-stream direction. That is to say,

$$\beta y v = g' \frac{\partial h}{\partial x}, \tag{2.1}$$

where x and y are pointing eastward and northward (Fig. 3), v is the velocity component in the y direction, β the familiar variation of the Coriolis parameter with latitude, g' the "reduced gravity" $g\Delta\rho/\rho$ (here, g is the gravitational acceleration and $\Delta\rho$ the density difference between the layers), and h is the total depth.

Introduction of the streamfunction ψ,

$$\partial\psi/\partial y = -uh; \quad \partial\psi/\partial x = vh \tag{2.2}$$

and multiplication of (2.1) by h gives

$$\beta y \frac{\partial\psi}{\partial x} = \frac{g'}{2}\frac{\partial}{\partial x}(h^2). \tag{2.3}$$

Integration of (2.3) in x from the wall to the current edge yields,

$$\beta y T = \frac{g'}{2}(h_e^2 - h_w^2), \tag{2.4}$$

where T is the net transport ($\psi_e - \psi_w$) of the jet (always positive), and h_e and h_w are the depths at the edge and wall, respectively. The subscripts "e" and "w" denote the "edge" and "wall." As mentioned, $h_e = H$ in the AM case and zero in our case.

Relation (2.4) can also be written as

$$h_w = \left(h_e^2 - \frac{2\beta y T}{g'}\right)^{1/2}, \tag{2.5}$$

which illustrates that, as demonstrated by AM, for a finite h_e (say, $h_e = H$), the jet can cross the equator and flow in the northern hemisphere because h_w is positive for $y \geq 0$ as long as $y < g'H^2/2\beta T$. As the AM jet proceeds northward in the northern hemisphere, its near-wall depth decreases (since y increases) until it ultimately vanishes. Then, the current cannot proceed farther to the north so that it turns offshore in analogy to the classical CHARNEY (1955) separation (see also PARSONS, 1969; OU and DE RUIJTER, 1986). The actual separation latitude may differ from that given by (2.5) (i.e. $y = g'H^2/2\beta T$) because at the separation point the current may no longer be geostrophic in the cross-stream direction. However, the actual separation point is within a deformation radius away from that given by (2.5) (MOORE and NIILER, 1974).

For our nonlinear frontal jet ($h_e = 0$), (2.5) gives

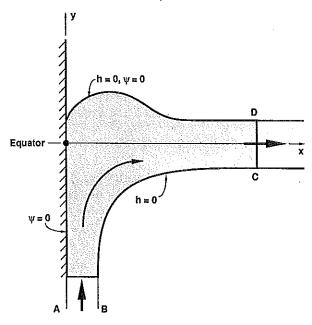$$h_w = \left(-\frac{2\beta y T}{g'}\right)^{1/2}, \tag{2.6}$$

Fig. 4.   A schematic view of the 1½ layer model. The wedge-like current separates from the coast
near the equator and forms a swift eastward jet. Detailed solutions are derived for the northward
and eastward jets away from the separating area (i.e. the regions in the vicinity of sections AB and
CD).

which is obviously valid only in the southern hemisphere ($y < 0$) because h_w must always
be positive. Namely, in our frontal case the classical mid-latitude separation shifts to the
equator ($y = 0$) and the current must turn offshore within a deformation radius away from
the equator (Fig. 4).

   In the classical mid-latitude separation case, it is impossible to solve for the detailed
downstream separated structure without solving for the detailed separation area* (MOORE
and NIILER, 1974). This impossibility results from the fact that the location of the
downstream flow is not known in advance. For our equatorial separation the situation is
different in that there is now only one eastward flow that can be connected to the upstream
flow via conservation of mass, potential vorticity and energy. This can be easily under-
stood by noting that our upstream northward-flowing frontal jet has a finite cross-section
so that downstream the separated current must also have a finite cross-section. Clearly,
thère is only one eastward jet with a finite cross-section; such a jet is symmetrical with
respect to the equator (Figs 4 and 5). It is worth mentioning here that a meandering
equatorial jet [of the kind discussed by MOORE and NIILER (1974) for the mid-latitude
separation] is impossible because a double-front current that alternately crosses the equator
from, say, north to south corresponds to alternate eastward–westward zonal flows.

---

* The problem can be considerably simplified by assuming that the current curvature is much greater than the
current width (OU and DE RUIJTER, 1986) but, even with this approximation, one cannot avoid solving for the
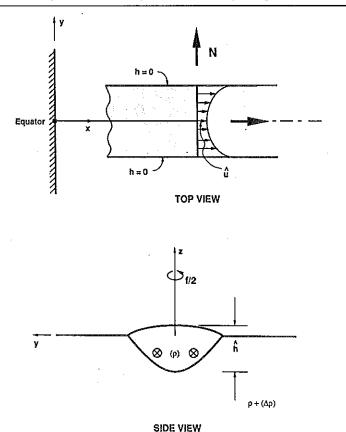transition area.

y

N

h = 0

Equator

x

h = 0

û

TOP VIEW

z

f/2

y

⊗ (ρ) ⊗

ĥ

ρ + (Δρ)

SIDE VIEW

Fig. 5. A schematic diagram of the eastward jet. Note that $\hat{u}$ and $\hat{h}$ are the speed and depth along the equator $(y = 0)$.

In view of the above, we shall adopt the upstream–downstream connection technique that is often used in rotating as well as nonrotating jet interaction studies. That is to say, we shall not solve for the detailed separation area but rather connect the far upstream and downstream regions via common conservation laws. The detailed solution of the separation area will be left as a subject for future investigation. The reader who wonders about the associated balance of momentum in the y direction is referred to Appendix A. Recall that in jet–wall interactions on a nonrotating plane and on an f plane (WHITEHEAD, 1985) the momentum integral provides an additional constraint which resolves the question of transport splitting resulting from the branching. Here, since no water can continue northward and, consequently, there is no branching, the momentum integral does not provide any additional constraint.

Detailed solution of the northward-flowing southern frontal jet

The solution presented in this subsection is similar to the western boundary current discussed by STOMMEL and ARONS (1972). Consider again the model shown in Fig. 3. An inviscid wedge-like current has a known structure at $y = y_u$. For simplicity, we shall

consider currents with zero potential vorticity. Recall, however, that the equatorial separation (2.6) is independent of the potential vorticity so that the results to be obtained can be extended to currents with finite potential vorticity.

The equations governing the northward jet are

$$\frac{\partial v}{\partial x} + \beta y = 0 \tag{2.7}$$

$$\frac{v^2}{2} + g'h = B \tag{2.8}$$

$$-\beta y v + g' \frac{\partial h}{\partial x} = 0 \tag{2.9}$$

$$\frac{\partial}{\partial x}(hu) + \frac{\partial}{\partial y}(hv) = 0, \tag{2.10}$$

where B is the Bernoulli constant (uniform for zero potential vorticity flows since the potential vorticity P is given by $P = dB/d\psi$). As mentioned earlier, the jet is in cross-stream geostrophic balance (2.9); the geostrophic relation (2.9) is introduced merely for convenience—it can be easily derived from the potential vorticity equation (2.7) and the Bernoulli integral (2.8).

The boundary conditions are

$$u = 0; \quad x = 0 \tag{2.11}$$

$$h = 0; \quad x = L(y) \tag{2.12}$$

$$\int_0^L vh dx = T, \tag{2.13}$$

where L is the current width and T is the transport. Condition (2.11) states that the wall is a streamline, (2.12) reflects the existence of the front and (2.13) states that the transport is known.

The solution of (2.7–2.10) in terms of T and B is

$$v = \sqrt{2}[B - (-2\beta y T g')^{1/2}]^{1/2} - \beta y x \tag{2.14}$$

and

$$h = \left(\frac{-2\beta y T}{g'}\right)^{1/2} + \frac{\beta y x \sqrt{2}}{g'}[B - (-2\beta y T g')^{1/2}]^{1/2} - \frac{\beta^2 x^2 y^2}{2g'}. \tag{2.15}$$

Note that, for every y_u, there is a threshold value for B necessary for the existence of the current $[B \geq (-2\beta y_u T g')^{1/2}]$. This results from the fact that there is a minimum amount of energy required for forcing the current toward the north. The width of the current $L(y)$ is obtained by setting $h = 0$ in (2.15),

$$L = \left[-(2B)^{1/2} + \sqrt{2}[B - (-2\beta y g' T)^{1/2}]^{1/2}\right]/\beta y, \tag{2.16}$$

which shows that L goes to infinity as $y \to 0$, indicating that the boundary current

approximation breaks down at the equator. This behavior is similar to that found in the classical mid-latitude separation case.

The eastward jet along the equator

For this area (see Fig. 5) the (one-dimensional) governing equations are

$$-\frac{\partial u}{\partial y} + \beta y = 0$$

$$\beta y u = -g' \frac{\partial h}{\partial y}$$

and the solution is

$$u = \hat{u} + \frac{\beta y^2}{2} \tag{2.17a}$$

$$h = \hat{h} - \frac{\beta \hat{u} y^2}{2g'} - \frac{\beta^2 y^4}{8g'}, \tag{2.17b}$$

where $\hat{u}$ and $\hat{h}$ are the velocity and depth along the equator $[\hat{u} = u(0); \hat{h} = h(0)]$. To determine $\hat{u}$ and $\hat{h}$ we connect the eastward equatorial jet to the upstream northward jet with the aid of the conservation of mass and energy. These give

$$T = 2\hat{u}\hat{h}\gamma - \frac{\beta\gamma^3}{3}\left(\frac{\hat{u}^2}{g'} - \hat{h}\right) - \frac{3\beta^2\hat{u}\gamma^5}{20g'} - \frac{\beta^3\gamma^7}{56g'} \tag{2.18}$$

$$B = \left[\hat{u} + \frac{\beta\gamma^2}{2}\right]^2 \Big/ 2, \tag{2.19}$$

where γ, half the width of the equatorial jet, is given by the condition $h = 0$ at $y = \pm\gamma$, i.e.

$$\gamma = \left[-\frac{2\hat{u}}{\beta} + \frac{2}{\beta}(\hat{u}^2 + 2g'\hat{h})^{1/2}\right]^{1/2}. \tag{2.20}$$

and T and B have the same values as those that are chosen for the northward jet.

The solution for $\hat{u}$, $\hat{h}$ and γ in terms of T and B cannot be easily derived analytically so it is preferred to present the solution in a graphical manner. We begin by illustrating the dependence of γ on $\hat{u}$ and $\hat{h}$ which is straightforward (Fig. 6). The dependence of $\hat{u}$ and $\hat{h}$ on T and B is not so simple. For each T and B there is at least one solution as shown in Figs 7 and 8. The answer to the uniqueness question associated with the narrow region where there are two solutions is not important for the present case because the corresponding values for B are below the threshold values of the northern jet.

Finally, it is worth pointing out that to find the northward and eastward jets corresponding to given values of T and B one proceeds as follows. First, one finds v, h, L and u for the northward jet from (2.14) to (2.16). Second, one turns to Fig. 7 to determine the (eastward) values of $\hat{u}$ and $\hat{h}$ corresponding to the (same) given values of T and B, and third, one finds the value of γ with the aid of Fig. 6. Lastly, (2.17) is used to obtain u and h
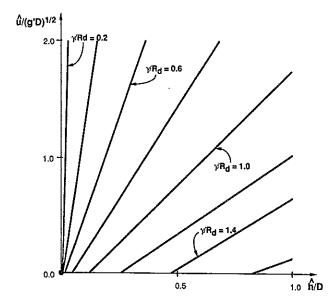
Fig. 6. The dependence of the eastward jet width (γ) on the central depth ($\hat{h}$) and speed ($\hat{u}$) according to (2.20). Note that D is the near-wall depth upstream [i.e. $D = h_w(y_u)$] and $R_d \equiv (g'D)^{1/4}/\beta^{1/2}$.

for the eastward jet. As mentioned in the caption of Fig. 8, all northward-flowing jets can be connected to eastward jets.

3. TWO-AND-ONE-HALF LAYER MODEL

We now consider a more realistic version of a northward-flowing western boundary current in the southern hemisphere. Instead of considering a mere wedge-like frontal flow we examine now a current with two moving layers (Figs 9 and 10). The core of the current (layer 1) is still a wedge but there is now an additional layer with a *finite* depth on the open ocean side (layer 2). The additional second layer is essentially equivalent to the single layer considered in the AM model. This model is of interest because one may initially suspect that the surrounding fluid may somehow carry the core northward allowing it to cross the equator. We shall see, however, that even though the surrounding flow may be strong, the core still cannot cross the equator.

Governing equations

The condition of no flow in the (third) lower layer is

$$g\eta_1 = g'(\xi_1 + \xi_2),\tag{3.1}$$

where η_1 is the free surface vertical displacement (measured upward from the undisturbed surface), ξ_1 and ξ_2 are the interfaces displacement (measured downward from the
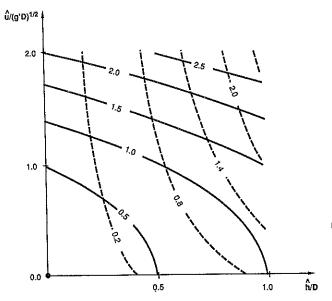
Fig. 7. The dependence of the transport $T/(g'D)^{1/2}DR_d$ (dashed lines) and Bernoulli function $B/(g'D)$ (solid lines) on the central speed and depth. Note that for a very narrow range of parameters the solution is not unique because the constant transport curves and the constant energy curves are expected to intersect twice. The range associated with this behavior is shown in Fig. 8. To find the solution graphically, one determines $\hat{h}$ and $\hat{u}$ for the known values of T and B and then proceeds to Fig. 6 to determine γ.

undisturbed level, Fig. 9). Here, the subscripts "1" and "2" correspond to the core and the moving environmental layer, respectively. The full shallow water governing equations are

$$u_1 \frac{\partial u_1}{\partial x} + v_1 \frac{\partial u_1}{\partial y} - \beta y v_1 + g' \left(\frac{\partial \xi_1}{\partial x} + \frac{\partial \xi_2}{\partial x} \right) = 0 \qquad (3.2)$$

$$u_2 \frac{\partial u_2}{\partial x} + v_2 \frac{\partial u_2}{\partial y} - \beta y v_2 + g' \frac{\partial \xi_2}{\partial x} = 0 \qquad (3.3)$$

$$\frac{\partial v_1}{\partial x} - \frac{\partial u_1}{\partial y} + \beta y = 0 \qquad (3.4)$$

$$\frac{\partial v_2}{\partial x} - \frac{\partial u_2}{\partial y} + \beta y = (H - \xi_1 + \xi_2) \frac{\beta y_p}{H} \qquad (3.5)$$

$$\frac{\partial}{\partial x} (\xi_1 u_1) + \frac{\partial}{\partial y} (\xi_1 v_1) = 0 \qquad (3.6)$$

$$\frac{\partial}{\partial x} [(H + \xi_2 - \xi_1)u_2] + \frac{\partial}{\partial y} [(H + \xi_2 - \xi_1)v_2] = 0, \qquad (3.7)$$

where condition (3.1) has been used in deriving (3.2)–(3.3), and H is the undisturbed depth of the intermediate layer (Fig. 9). A simple qualitative analysis of (3.2)–(3.7)
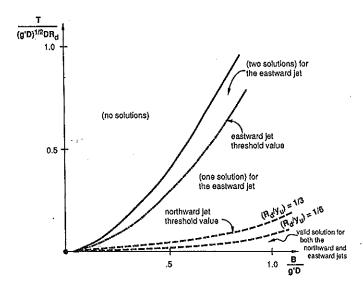
Fig. 8. The various regimes associated with the solutions. The threshold value of B for the eastward jet is shown by the dashed–dotted line; the region of no solution corresponds to a situation where there is not enough energy to force the given transport along the equator. (The uniqueness question associated with the narrow region where there are two solutions is beyond the scope of this study. Its resolution probably requires a detailed analysis of the separation region.) The threshold value for the northward jet (dashed lines) is given by $[T/(g'D)^{1/2}DR_d] = 1/2(R_d/y_u)(B/g'D)^2$; since $(R_d/y_u) \ll 1$ it follows that for every northward jet there exists a corresponding eastward jet. That is to say, the threshold value of B is much larger for the northward jet than it is for the eastward jet.

illustrates that the frontal current (layer 1) cannot cross the equator. Specifically, from (3.3) one finds that, in a boundary current, $\partial\xi_2/\partial x$ vanishes when $y = 0$ so that, in view of (3.2), $\partial\xi_1/\partial x$ also vanishes at the equator. This implies that, as in the $1\frac{1}{2}$ layer case, the core has no cross-sectional area at the equator and, therefore, cannot cross it. In what follows we shall solve the set (3.2)–(3.7) in detail and show that, as the above qualitative analysis suggests, the core cannot cross the equator.

Note that, initially, we shall take the potential vorticity of the intermediate layer to be negative and uniform; it equals $\beta y_p/H$, where $y_p(<0)$ is the "potential vorticity latitude" of the current. Later on we shall consider positive potential vorticities. The boundary conditions and constraints are

$$u_1 = 0; \quad x = 0 \tag{3.8}$$

$$u_2 = 0; \quad x = 0 \tag{3.9}$$

$$\xi_1 = 0; \quad x = L_1(y) \tag{3.10}$$

$$\xi_2 = 0; \quad x = L_2(y) \tag{3.11}$$

$$v_2 = 0; \quad x = L_2(y), \tag{3.12}$$

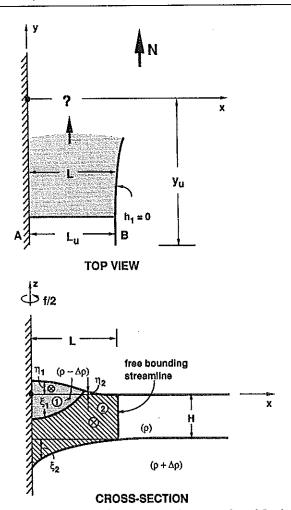$$T_1 = \int_0^{L_1} u_1 h_1 dx \tag{3.13a}$$

Fig. 9. A schematic diagram of the $2\frac{1}{2}$ layer model. The two northward-flowing layers consist of a wedge-like core (shaded) and an intermediate layer with a finite depth on the ocean side (hatched). As in the single layer reduced-gravity model, there is no mathematical difference between a surface core and an intermediate core (Fig. 10). It is shown in the text that only the hatched fluid (i.e. the nonfrontal intermediate layer) can cross the equator.

$$T_2 = \int_0^{L_2} u_2 h_2 \, dx. \tag{3.13b}$$

The first two conditions (3.8)–(3.9) state that the wall is a streamline. Condition (3.10) reflects the vanishing of the upper layer depth, whereas conditions (3.11 and 3.12) are related to the free streamline that bounds the intermediate layer. As in AM, we chose the velocity to be zero along the free bounding streamline even though there is really no requirement to do so. Strictly speaking, since the model is inviscid it is sufficient to require the velocity to be *constant* along this line.

Expansions

To solve the problem the following scales are introduced:

$$x^* = \frac{x}{\varepsilon^{1/4} R_d}; \quad y^* = \frac{\varepsilon^{1/4} y}{R_d}; \quad h^* = \frac{h}{D}; \quad \varepsilon = \left(\frac{R_d}{y_u}\right)^4 \ll 1$$

$$(3.14)$$

$$u^* = \frac{u}{\varepsilon^{1/2} \beta R_d^2}; \quad v^* = \frac{v}{\beta R_d^2}; \quad R_d = \frac{(g'D)^{1/4}}{\beta^{1/2}}.$$

Here, R_d is the deformation radius based on the upstream near-wall depth (D) and β. With these scalings the current has the structure of a jet and,

$$x^*, y^* \sim O(1); \quad u^*, v^* \sim O(1); \quad h^* \sim O(1); \quad \varepsilon \ll 1.$$

We also impose the special conditions $(D/H) \sim O(\varepsilon), \xi_1^* \sim O(\xi_2^*) \sim O(\varepsilon)$ and $v_2^* \sim O(1)$ which imply that the second layer is much deeper than the core. Recall that, because cross-section "u" is situated at some distance from the equator, the x length scale is much smaller than the Rossby radius; this reflects the presence of $\varepsilon^{1/4}$ in the scaling for x. Also, note that ε is given since both R_d and y_u are known. Finally, it should be pointed out that the above scales are identical to those which, in a rigorous manner, yield the jet equations presented earlier in Section 2.

Using these nondimensional variables and common expansions in powers of ε one finds the following zeroth-order equations,

$$-y^* v_1^{(0)} + \frac{\partial \xi_1^{(0)}}{\partial x^*} + \frac{\partial \xi_2^{(0)}}{\partial x^*} = 0 \qquad (3.15)$$
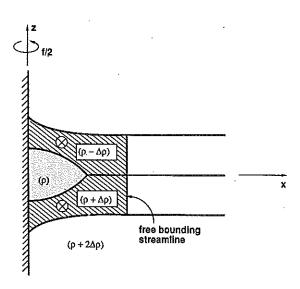

Fig. 10. A cross-section of a layered model mathematically analogous to the $2\frac{1}{2}$ layer model shown in Fig. 9. The difference between the two situations is that in the former the core (i.e. the frontal current) is on the surface whereas in the present the core is submerged. The uppermost and lowermost layers are at rest.

$$-y^* v_2^{(0)} + \frac{\partial \xi_2^{(0)}}{\partial x^*} = 0 \tag{3.16}$$

$$\frac{\partial v_1^{(0)}}{\partial x^*} + y^* = 0 \tag{3.17}$$

$$\frac{\partial v_2^{(0)}}{\partial x^*} + y^* = y_p^* \tag{3.18}$$

$$\frac{\partial}{\partial x^*} \left(\xi_1^{(0)} u_1^{(0)} \right) + \frac{\partial}{\partial y^*} \left(\xi_1^{(0)} v_1^{(0)} \right) = 0 \tag{3.19}$$

$$\frac{\partial u_2^{(0)}}{\partial x^*} + \frac{\partial v_2^{(0)}}{\partial y^*} = 0. \tag{3.20}$$

With these approximations the deep intermediate layer is not affected by the core layer (see 3.16 and 3.18) but the core is strongly affected by the fluid underneath 3.15. *Note that, even though the intermediate layer is much deeper than the core, the speeds in both moving layers are of* $O(1)$.

The zeroth-order boundary conditions and constraints are

$$u_1^{(0)} = u_2^{(0)} = 0; \quad x^* = 0 \tag{3.21a}$$

$$\xi_1^{(0)} = 0; \quad x^* = L_1^{(0)}(y^*) \tag{3.21b}$$

$$\xi_2^{(0)} = 0; \quad x^* = L_2^{(0)}(y^*) \tag{3.21c}$$

$$v_2^{(0)} = 0; \quad x^* = L_2^{(0)}(y^*), \tag{3.21d}$$

$$T_1^* = \int_0^{L_1^{(0)}} u_1^{(0)} h_1^{(0)} dx^*; \quad x^* = L_1^{(0)}(y^*) \tag{3.21e}$$

$$T_2^* = \int_0^{L_2^{(0)}} u_2^{(0)} h_2^{(0)} dx^*; \quad x^* = L_2^{(0)}(y^*), \tag{3.21f}$$

where T_1 has been scaled with $\varepsilon^{1/4} \beta R_d^3 D$ and T_2 with $\beta R_d^3 H \varepsilon^{1/4}$. The derivation of the detailed zeroth-order solution is presented in Appendix B.

Properties of the solution

The solution $L_1^{(0)}$ and $L_2^{(0)}$ for a cross-section in the southern hemisphere ($y^* = -1$) is found from (B11) and (B12) and is shown in Figs 11 and 12. It is important to realize that solutions can be found only for a limited range of parameters; there is some range in the T_1^*, T_2^* plane for which there is no boundary current solution. Note that the width of the core (Fig. 12) increases as the equator is approached; ultimately, the boundary current approximation breaks down. This increase in width can be traced to the *local* deformation radius which increases with decreasing distance to the equator. The width of the intermediate layer, on the other hand, decreases as the equator is approached because here the depth is constant (to zeroth-order) and the velocity increases with decreasing distance to the equator.
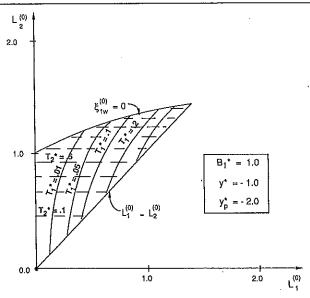
Fig. 11. The solution of the 2½ layer model for a cross-section in the *southern hemisphere*. Both the core and the intermediate layer have negative potential vorticity $\beta y_p/H$ (where $y_p < 0$). For each T_1^* (solid lines) and T_2^* (dashed lines) there is one core width ($L_1^{(0)}$) and one intermediate layer ($L_1^{(0)}$).
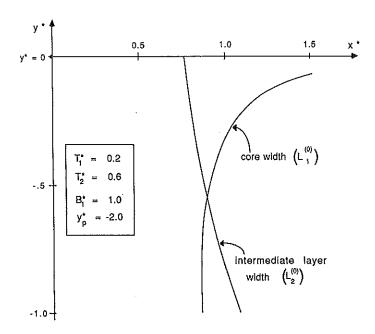

Fig. 12. The width of the core and the intermediate layer in the 2½ layer model. This southern hemisphere flow corresponds to a uniform negative potential vorticity ($y_p^* = -2$) associated with zero speed along the free separating streamline. Note that the boundary current approximation breaks down in the vicinity of the equator because the core's width varies rapidly with y^*.
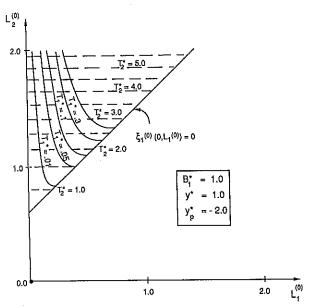
Fig. 13. The same as in Fig. 11 but for a cross-section in the *northern hemisphere* ($y^* > 0$). This solution indicates that a system consisting of a northward-flowing wedge embedded in an intermediate layer *can exist* in the northern hemisphere.

We shall now proceed and discuss the solution of $L_1^{(0)}$ and $L_2^{(0)}$ for the northern hemisphere (Fig. 13). Recall that, as illustrated earlier, a northward-flowing single wedge-like current *cannot exist* in the northern hemisphere so that we might have expected that there would not be *any* solution for $L_1^{(0)}$ and $L_2^{(0)}$ in the northern hemisphere. Figure 13 shows, however, that, in contrast to the reduced-gravity single layer model, there *are admissible solutions* for northward-flowing jets in the northern hemisphere. This implies that a system consisting of a northward wedge-like core embedded in a northward current can exist in the northern hemisphere.

At first sight one may tend to interpret the above result as an indication that such a system can perhaps somehow cross the equator. A careful examination of the regime for which the solutions are valid in both hemispheres (Fig. 14) reveals, however, that, as our earlier qualitative analysis indicates, this is not the case. Figure 14 illustrates that the regions of validity in the two hemispheres do not overlap (except for $T_1^* = 0$, indicating that one cannot find any nonzero transports (T_1^* and T_2^*) for which there is a solution valid in *both hemispheres simultaneously*. One concludes, therefore, that, even if there exists an adjacent jets system in the northern hemisphere, it could not possibly have originated in the southern hemisphere. Namely, adjacent jets cannot cross the equator as one unit.

The picture that emerges from the above analysis is as follows. When adjacent jets approach the equator from the south they cannot cross the equator as one unit. Consequently, the core separates from the wall (Fig. 15) and forms an eastward jet; the intermediate jet crosses the equator in the manner illustrated by AM and Fig. 2. It is easy to show analytically that the structure of the separated eastward jet originating in the core is identical to that of the eastward jet in the single layer model. Similarly, the structure of the intermediate jet in the northern hemisphere is identical to the structure that it had in

the southern hemisphere except that y^* is now positive. This results from the fact that to zeroth-order the core does not affect the intermediate jet. Note that since $\xi_1^* \sim O(\xi_2^*) \sim O(\varepsilon)$, our approximation allows the interface of the core to surface but it does not allow for a surfacing interface of the intermediate layer. Consequently, the familiar mid-latitude separation is filtered out.

Finally, it should be pointed out that the above results are not sensitive to the choice of potential vorticity. However, when the potential vorticity is taken to be positive instead of negative, the velocity along the free bounding streamline associated with the intermediate jet must be taken to be positive and nonzero. The associated discontinuity is not unusual in inviscid models although the flow might be locally unstable. The results for the positive potential vorticity case do not provide any new insights and, therefore, are not presented.

4. APPLICATION TO THE NEW GUINEA COASTAL UNDERCURRENT

So far, only a few observations have focused on cross equatorial jets in the Pacific Ocean. This is unfortunate because the matter is obviously important to the global meridional heat flux and the establishment of the equatorial undercurrent. The analyses of TSUCHIYA (1968) and ROUGERIE (1969) are exceptions to this lack of attention. By tracing oxygen concentrations in the western tropical Pacific, TSUCHIYA (1968) concluded that the
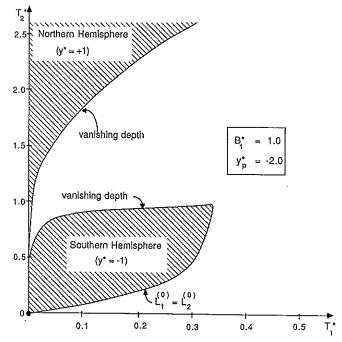

Fig. 14.   The validity regime for the $2\frac{1}{2}$ layer model. As before, T_1^* and T_2^* correspond to the transport in the core and the intermediate layer, respectively. For each hemisphere there exists a single region for which there is a physically valid solution. This indicates that the system described by the $2\frac{1}{2}$ layer model can exist in *both* hemispheres. However, the regions *do not overlap*, indicating that, as a unit, the flow cannot cross the equator because one cannot find any T_1^* and T_2^* that would give a solution valid in both hemispheres *simultaneously*.
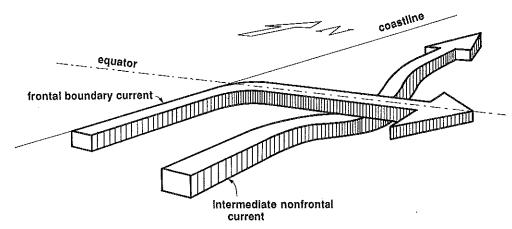
Fig. 15. A schematic view of the flows associated with the $2\frac{1}{2}$ layer model. The core (i.e. the frontal current) separates from the wall along the equator and turns eastward whereas the intermediate (nonfrontal) layer continues northward and crosses the equator with no apparent difficulty.

main source of the undercurrent is the water from the western South Pacific (Fig. 2). LINDSTROM *et al.* (1987) confirmed this hypothesis using direct observations. The foregoing theory suggests that in almost all oceans some waters will be blocked by the equator. Namely, even though the extension of the $2\frac{1}{2}$ layer model to a continuously stratified ocean is not trivial, it is reasonable to assume that most boundary jets will have some sort of a wedge-like core bounded by a front on the open ocean side. With a willingness to accept the concept that the core of the actual current is wedge-like one arrives at the conclusion that our present theory for a subsurface core (Fig. 10) may explain the pattern shown in Fig. 2. The theory predicts that upon approaching the equator from the south the wedge-like core of the western boundary current will separate and turn offshore to form an eastward jet (Fig. 15).

It should be pointed out that since the western boundary in the Pacific is actually porous, there probably is some leakage to the left of the equatorial separation area. This may provide an alternative explanation for the fact that relatively high oxygen concentrations are not found near the coast in the northern hemisphere. However, it does not provide an explanation for the high oxygen concentration along the equator.

REFERENCES

ANDERSON D. L. T. and D. W. MOORE (1979) Cross-equatorial inertial jets with special relevance to very remote forcing of the Somali Current. *Deep-Sea Research*, **26**, 1–22.

Charney J. G. (1955) The Gulf Stream as an inertial boundary layer. *Proceedings of the National Academy of Science*, **41**, 731–740.

Csanady G. T. (1985) A zero potential vorticity model of the North Brazilian Coastal Current. *Journal of Marine Research*, **43**, 553–579.

Eriksen C. and E. Katz (1987) Equatorial dynamics. *Review of Geophysics and Space Physics*, **21**, 217–226.

Kawase M. (1987) Establishment of deep ocean circulation driven by deep-water production. *Journal of Physical Oceanography*, **17**, 2294–2317.

Lindstrom E., R. Lukas, R. Fine, E. Firing, S. Godfrey, G. Meyers and M. Tsuchiya (1987) The Western Equatorial Pacific Ocean Circulation Study. *Nature*, **330**, 533–537.

McCreary J., Jr (1985) Modeling equatorial ocean circulation. *Annual Review of Fluid Mechanics*, **17**, 359–409.

Moore D. W. and P. Niiler (1974) A two-layer model for the separation of inertial boundary currents. *Journal of Marine Research*, **32**, 457–484.

Ou H. and W. De Ruijter (1986) Separation of an inertial boundary current from a curved coastline. *Journal of Physical Oceanography*, **16**, 280–289.

Parsons A. T. (1969) A two-layer model of Gulf Stream separation. *Journal of Fluid Mechanics*, **39**, 511–528.

Philander S. G. (1985) Tropical oceanography. *Advances in Geophysics*, **28**, 461–477.

Rougerie F. (1969) Sur un noyar a forte teneur en oxygène dans la partie inférieure du courant de Cromwell. *Cahiers O.R.S.T.O.M., Série Océanographic*, **7**, 26-27.

Stommel H. and A. Arons (1972) On the abyssal circulation of the world ocean—V. The influence of bottom slope on the broadening of inertial boundary currents. *Deep-Sea Research*, **19**, 707–718.

Tsuchiya M. (1968) *Upper waters of the intertropical Pacific Ocean*. The Johns Hopkins Oceanographic Studies, No. 4. The Johns Hopkins Press, Baltimore.

Whitehead J. A. (1985) The deflection of a baroclinic jet by a wall in a rotating fluid. *Journal of Fluid Mechanics*, **157**, 79–93.

APPENDIX A: GENERAL STRUCTURE OF THE SEPARATED CURRENT

The purpose of this Appendix is to demonstrate that the separation shown in Fig. 3 is consistent with the flow-force balance associated with other jet–wall interactions (e.g. Whitehead, 1985). Since the jet does not penetrate into the northern hemisphere one may wonder how is the flow-force balanced in the y direction. Specifically, because the current is bounded by a front from the north, it is not *a priori* obvious what is the force that could balance the northward flow-force associated with the northward-flowing jet. To answer this question, the momentum equation in the y direction is multiplied by h and integrated over the area shown in Fig. 4.

$$\iint \left[hu\frac{\partial v}{\partial x} + hv\frac{\partial v}{\partial y} + \beta yuh + \frac{g'}{2}\frac{\partial}{\partial y}(h^2) \right] \mathrm{d}x\mathrm{d}y = 0. \tag{A1}$$

Using the continuity equation, (2.27) can also be written as

$$\iint \left[\frac{\partial}{\partial x}(huv) + \frac{\partial}{\partial y}(hv^2) - \beta y\frac{\partial \psi}{\partial y} + \frac{g'}{2}\frac{\partial}{\partial y}(h^2) \right] \mathrm{d}x\mathrm{d}y = 0$$

which can be further simplified using Stokes' theorem to

$$\oint huv\mathrm{d}y - \oint \left(hv^2 + \frac{g'h^2}{2} \right) \mathrm{d}x - \iint \beta \left[\frac{\partial}{\partial y}(y\psi) - \psi \right] \mathrm{d}x\mathrm{d}y = 0. \tag{A2}$$

Taking into account the geometry of the integrated area, (A2) can be easily reduced to

$$\int_A^B \left(hv^2 + \frac{g'h^2}{2} - \beta y\psi \right) \mathrm{d}x + \beta \iint \psi \mathrm{d}x\mathrm{d}y + \beta \int_B^C y\psi \mathrm{d}x = 0. \tag{A3}$$

Furthermore, since the flow away from the separation area is geostrophic, the sum of the second and third terms in the first integral vanish and we have,

$$\int_A^B hv^2 \mathrm{d}x + \beta \iint \psi \mathrm{d}x\mathrm{d}y + \beta \int_B^C y\psi \mathrm{d}x = 0. \tag{A4}$$

Note that, due to the geometry, the first term is always positive whereas the second and third are always negative.

One concludes that the positive northward flow-force associated with the upstream jet (the first term) is balanced by negative southward forces generated by β (the second and third terms). This completes our demonstration of the consistency of our general separation process.

APPENDIX B: ZEROTH ORDER SOLUTION OF THE $2\frac{1}{2}$ LAYER MODEL

The general solution of (3.17)–(3.18) is

$$v_1^{(0)} = -y^*x^* + V_{1w}^{(0)} \tag{B1}$$

$$v_2^{(0)} = -(-y_p^* + y^*)x^* + V_{2w}^{(0)}, \tag{B2}$$

which together with (3.10) and (3.15) give,

$$\xi_2^{(0)} = -y^*(-y_p^* + y^*)(x^*)^2/2 + V_{2w}^{(0)}x^*y^* + \xi_{2w}^{(0)} \tag{B3}$$

$$\xi_1^{(0)} = y^*[(V_{1w}^{(0)} - V_{2w}^{(0)})x^* - y_p^*(x^*)^2/2] + \xi_{1w}^{(0)}. \tag{B4}$$

Substitution of the boundary conditions and constraints (3.21b)–(3.21f) into (B1)–(B4) gives five algebraic equations with six unknowns ($L_1^{(0)}$, $L_2^{(0)}$, $V_{1w}^{(0)}$, $V_{2w}^{(0)}$, $\xi_{1w}^{(0)}$, $\xi_{2w}^{(0)}$). As before, specifying the transports and potential vorticity is not sufficient and an additional variable must be specified in order to solve the problem.

For convenience, we again choose to specify the core's Bernoulli function B_1^* because, aside from (T_1^*) and (T_2^*), it is the only variable that does not vary with y^*. In view of this we have

$$-y^*(-y_p^* + y^*)(L_2^{(0)})^2/2 + V_{2w}^{(0)}L_2^{(0)}y^* + \xi_{2w}^{(0)} = 0 \tag{B5}$$

$$y^*[(V_{1w}^{(0)} - V_{2w}^{(0)})L_1^{(0)} - y_p^*(L_1^{(0)})^2/2] + \xi_{1w}^{(0)} = 0 \tag{B6}$$

$$-(-y_p^* + y^*)L_2^{(0)} + V_{2w}^{(0)} = 0 \tag{B7}$$

$$T_1^* = (y^*)^2(L_1^{(0)})^4 y_p^*/8 - \frac{(L_1^{(0)})^3}{3}y^*[y^*(V_{1w}^{(0)} - V_{2w}^{(0)}) + V_{1w}^{(0)}y_p^*/2]$$

$$+ \frac{(L_1^{(0)})^2}{2}[y^*(V_{1w}^{(0)} - V_{2w}^{(0)}) - \xi_{1w}^{(0)}] + V_{1w}^{(0)}\xi_{1w}^{(0)}L_1^{(0)}. \tag{B8}$$

$$T_2^* = -\frac{(L_2^{(0)})^2}{2}(-y_p^* + y^*) + V_{2w}^{(0)}L_2^{(0)} \tag{B9}$$

$$B_1^* = \frac{(V_{1w}^{(0)})^2}{2} + \xi_{1w}^{(0)} + \xi_{2w}^{(0)}, \tag{B10}$$

where (3.1) has been used in the derivation of (B10). Substitution of $\xi_{1w}^{(0)}$, $\xi_{2w}^{(0)}$, $V_{2w}^{(0)}$ and $V_{1w}^{(0)}$ from (B6), (B5), (B7) and (B10) into (B8) and (B9) gives the following equations for $L_1^{(0)}$ and $L_2^{(0)}$,

$$T_1^* = -\frac{1}{24}\left\{y^*\left[4y_p^*(L_1^{(0)})^2(2L_1^{(0)} - 3L_2^{(0)})[(L_2^{(0)} - L_1^{(0)})^2y^*(-y_p^* + y^*) + 2B_1^*]^{1/2}\right.\right.$$

$$\left. + 24B_1^*(L_1^{(0)})^2\right] + (y^*)^2[4L_1^{(0)2}(5L_1^{(0)} - 3L_2^{(0)})(L_2^{(0)} - L_1^{(0)})^2y^*(-y_p^* + y^*)$$

$$+ 2B_1^*]^{1/2} - y_p^*(L_1^{(0)})^2[12(L_2^{(0)})^2 - 32L_1^{(0)}L_2^{(0)}$$

$$\left. + 17(L_2^{(0)})^2] + 4(y^*)^3(L_1^{(0)})^2[3(L_2^{(0)})^2 - 8L_1^{(0)}L_2^{(0)} + 5(L_1^{(0)})^2]\right\} \tag{B11}$$

and

$$T_2^* = (L_2^{(0)})^2(-y_1^* + y^*)/2. \tag{B12}$$